

LIGHT-ASSISTED DRYING (LAD) FOR ANHYDROUS PRESERVATION OF  
BIOLOGICS: PROCESSING SAMPLE VOLUMES COMPARABLE TO A  
THERAPEUTIC DOSE

by

Daniel Patterson Furr

A thesis submitted to the faculty of  
The University of North Carolina at Charlotte  
in partial fulfillment of the requirements  
for the degree of Master of Science in  
Applied Physics

Charlotte

2022

Approved by:

---

Dr. Susan Trammell

---

Dr. Donald Jacobs

---

Dr. Yong Zhang

©2022  
Daniel Patterson Furr  
ALL RIGHTS RESERVED

## ABSTRACT

DANIEL PATTERSON FURR. Light-assisted drying (LAD) for anhydrous preservation of biologics: processing sample volumes comparable to a therapeutic dose. (Under the direction of DR. SUSAN TRAMMELL)

Protein-based products have been developed to treat a range of conditions and are used in vaccines and assays. A challenge in the development of these products is maintaining the protein in the folded state during processing and storage. The most common method of stabilizing proteins for storage is lyophilization (freeze drying). However, this process remains expensive and many proteins that are lyophilized must be refrigerated or frozen to maintain functionality. Cold-chain storage can be challenging and expensive for the transportation and storage of biologics, especially in low-resource settings. Recent research has demonstrated that anhydrous preservation in a trehalose amorphous solid matrix offers an alternative to freeze drying for the preservation of biologics. We have previously described a new processing technique, light assisted drying (LAD), to create trehalose preservation matrices of small volume (40  $\mu\text{L}$ ) samples. LAD uses illumination by near-infrared laser light to selectively heat water and speed dehydration. In this study we apply the LAD technique to large volume samples (250  $\mu\text{L}$ ) that are more comparable to therapeutic doses. A model protein, lysozyme, was LAD processed then stored for 1 month. The end moisture content of samples was determined immediately after processing and then again after storage. The thermal histories of samples were monitored during processing to determine the optimal drying time. The trehalose matrix was characterized using polarized light imaging to determine if crystallization occurred during storage, damaging embedded proteins. Raman spectroscopy was used to determine the distribution of water content. Karl-Fischer (KF) Titration was used to analyze the actual water content of the samples. These studies indicate that LAD can effectively stabilize large volume samples.

## DEDICATION

To mom, dad, my grandparents, and my brother, thank you all for the love and support. I would have never made it this far without you. And to the Mint Hill squad (you know who you are), thanks for putting up with me all these years.

## ACKNOWLEDGEMENTS

I would like to sincerely thank Dr. Trammell for believing in me and helping me achieve my academic goals. One could not ask for a better advisor. To Anteneh Tsegaye, Maddie Kern, Gunnar Olson, Tang Ye, and Riley McKeough, thank you for your collaboration and aid. I would not have been able to accomplish my research without your support. To Cobey McGinnis, you have been a great mentor and friend and I would like to sincerely thank you for all you have done to help me throughout the years.

## TABLE OF CONTENTS

LIST OF TABLES	vii
LIST OF FIGURES	ix
LIST OF ABBREVIATIONS	xi
CHAPTER 1: INTRODUCTION	1
1.1. Motivation	1
1.2. Anhydrous Preservation	2
1.3. This Study	7
CHAPTER 2: METHODS	10
2.1. LAD Processing	10
2.2. Polarized Light Imaging	12
2.3. Raman Spectroscopy	13
2.4. Karl Fischer Titration	14
CHAPTER 3: Results and Analysis	15
3.1. End Moisture Contents	15
3.2. Thermal Histories	17
3.3. Polarized Light Imaging	21
3.4. Raman Spectroscopy	27
3.5. Karl Fischer Titration	35
CHAPTER 4: Discussion and Conclusions	38
REFERENCES	41

## LIST OF TABLES

TABLE 3.1: A summary of the average EMC of samples immediately after LAD processing, after storage at room temperature, and after storage at 4° C. Includes the change in EMC before and after storage. All values measured in gH <sub>2</sub> O/gDryWeight.	15
TABLE 3.2: A summary of the ANOVA test results for the EMC data.	17
TABLE 3.3: A summary of the Tukey-Kramer test results for the EMC data.	17
TABLE 3.4: Spearman correlation coefficients between EMC and maximum temperature, and EMC and change in temperature.	21
TABLE 3.5: Crystal growth of samples after 1-month storage at 4°C. Crystal growth is measured in pixels.	25
TABLE 3.6: Crystal growth of samples after 1-month storage at room temperature (20°C). Crystal growth is measured in pixels.	26
TABLE 3.7: A summary of the ANOVA test results for the PLI data.	26
TABLE 3.8: A summary of the Tukey-Kramer test results for the PLI data.	26
TABLE 3.9: EMCs and Average Line Ratios for All Samples. The EMC is given in units of gH <sub>2</sub> O/gDryWeight.	28
TABLE 3.10: A summary of the ANOVA test results for the mean values of the 3:1 and 3:2 peak ratios.	29
TABLE 3.11: A summary of the Tukey-Kramer test results for the mean values of the 3:1 peak ratios.	29
TABLE 3.12: A summary of the Tukey-Kramer test results for the mean values of the 3:2 peak ratios.	29
TABLE 3.13: The COV as a function of position for the 2:1, 3:1 and 3:2 line ratios for all samples. The EMC of the sample at the time of testing is given in units of gH <sub>2</sub> O/gDryWeight.	36

TABLE 3.14: The water content of samples tested using KF Titration.  
The EMC is given in gH<sub>2</sub>O/gDryWeight. The theoretical glass transition temperature is given in °C.

## LIST OF FIGURES

FIGURE 1.1: Scanning electron micrograph of a tardigrade in (A) its active state and (B) its desiccated state. <sup>20</sup>	3
FIGURE 1.2: A comparison between a protein stabilized through hydrogen bonds (bottom path) and a non-protected protein (top path) during desiccation. <sup>27</sup>	5
FIGURE 1.3: A pictorial representation of the mechanical entrapment hypothesis. The trehalose (purple) is completely surrounding the protein (grey and red). <sup>28</sup>	6
FIGURE 1.4: Theoretical representation of what the broken glass hypothesis would look like. The trehalose (light blue) is preferentially binding at specific parts of the protein. A few trehalose molecules (dark blue) are shown for size comparison. <sup>28</sup>	6
FIGURE 1.5: Dependence of glass transition temperature of a trehalose-water mixture on end moisture content of the sample, adapted from the Gordon-Taylor equation for binary solutions of polymers. <sup>34</sup>	8
FIGURE 2.1: LAD experimental set-up within a controlled low relative humidity chamber. A sample is illuminated with a near-IR laser. The temperature of the sample is monitored during processing using the thermal camera. <sup>15</sup>	11
FIGURE 2.2: Polarized light imaging setup. Samples were placed on a borosilicate glass coverslip between the polarizer and analyzer then imaged from above. <sup>16</sup>	12
FIGURE 2.3: Representative image showing the five locations where the Raman spectrum was obtained for each sample. $R$ is the radius of the sample. The average radius of the samples tested was 7.5mm.	13
FIGURE 3.1: Thermal histories for the samples stored at 4°C (a) and room temperature (b).	18
FIGURE 3.2: EMCs of samples as a function of maximum temperature reached during processing.	20
FIGURE 3.3: EMCs of samples as a function of change in temperature during processing.	20

- FIGURE 3.4: PLI of a LAD processed sample where (a-b) were taken immediately after LAD processing and (c-d) were taken after 1 month of storage at 4°C. Images a and c were taken with the polarizer and analyser at the same angle. Images b and d are the crossed-polarizer images and areas of crystallization should appear white in these images. 22
- FIGURE 3.5: PLI of a LAD processed sample where (a-b) were taken immediately after LAD processing and (c-d) were taken after 1 month of storage at room temperature. Images a and c were taken with the polarizer and analyser at the same angle. Images b and d are the crossed-polarizer images and areas of crystallization should appear white in these images. 23
- FIGURE 3.6: Representative Raman spectrum for a LAD processed sample. Peaks 1 and 2 are due to trehalose and peak 3 contains contributions from both water and trehalose. 30
- FIGURE 3.7: Line ratios as a function of position for LAD processed samples. These samples were not stored and Raman spectroscopy was performed immediately after LAD processing. The 3to1Ratio axis represents the water to trehalose comparison and the 2to1Ratio axis represents the trehalose to trehalose comparison. 31
- FIGURE 3.8: Line ratios as a function of position for LAD processed samples stored for one month at 4°C. The 3to1Ratio axis represents the water to trehalose comparison and the 2to1Ratio axis represents the trehalose to trehalose comparison. 32
- FIGURE 3.9: Line ratios as a function of position for LAD processed samples stored for one month at room temperature. The 3to1Ratio axis represents the water to trehalose comparison and the 2to1Ratio axis represents the trehalose to trehalose comparison. 33

## LIST OF ABBREVIATIONS

ANOVA Analysis of Variance

COV Coefficient of Variation

CW Continuous Wave

DS Drying Solution

EMC End Moisture Content

FWHM Full Width Half Maximum

KF Karl-Fischer

LAD Light Assisted Drying

NA Numerical Aperture

PBS Phosphate Buffer Solution

PLI Polarized Light Imaging

RH Relative Humidity

$T_g$  Glass Transition Temperature

## CHAPTER 1: INTRODUCTION

### 1.1 Motivation

The use of biologics in diagnostics and therapeutics has increased dramatically since the introduction of the first protein therapeutic, human insulin, more than thirty years ago.<sup>1</sup> Since then protein therapeutics have been developed to treat diseases ranging from arthritis to cancer, and protein diagnostics, which contain immobilized capture proteins, have been developed for the detection of diseases.<sup>2</sup> A challenge in the development of protein-based products is maintaining the protein in the folded state during processing and storage, as the three-dimensional structure of the protein is often responsible for its functional activity.<sup>3-5</sup> Previous research has shown that light-assisted drying (LAD) has the potential to provide a novel method of preservation for room temperature storage of protein-based drugs and diagnostics. LAD works by forming an amorphous material around the proteins that aids in maintaining the protein's three-dimensional structure, and thus its functionality.

The current method most widely used for the storage of proteins and other biologics is freeze drying, or lyophilization. Freeze-drying has achieved long-term preservation at supra-zero temperatures for some biological products.<sup>6-9</sup> Lyophilization is normally done in two steps, first the protein solution is frozen then the frozen water and the non-frozen bound water are removed from the sample under vacuum. This process is not only lengthy and expensive but it can generate a variety of freezing and drying stresses, such as pH changes and the formation of ice crystals, which can cause the protein to undergo unwanted conformational changes.<sup>10,11</sup> Many proteins denature to various degrees during the lyophilization process, especially at low concentrations. In many cases this loss of structure is non-reversible. For example it has been shown

that freeze drying results in the complete loss of phosphofructokinase and lactate dehydrogenase activity in the absence of stabilizers.<sup>12</sup> In order to protect the protein and reduce the risk of denaturation during lyophilization, chemical additives known as cryoprotectants must be added to the solution.<sup>13</sup> These cryoprotectants are often not bio-compatible but must be used in order preserve the protein.<sup>10</sup> Proteins that are successfully freeze dried can be stored as long as one year or more; however, most of these proteins must be stored at or below 4°C.<sup>14</sup> This can make the transportation of protein-based products challenging and can be difficult or impossible in low resource settings due to a lack of available infrastructure.

We have previously developed a novel process that provides a quick, relatively inexpensive processing method to stabilize proteins and other biologics for anhydrous preservation at supra-zero temperatures.<sup>15,16</sup> This process utilizes a glass-forming, sugar-based protectant to create a vitrified matrix suitable for storage at elevated temperatures. Near infrared light is used to control the drying of the sample.

## 1.2 Anhydrous Preservation

Anhydrous, or dry state, preservation is the process of removing water from a solution that contains glass forming substances, such as disaccharide trehalose. An amorphous solid is a non-crystalline solid such as a glass, where the atoms and molecules of the solid do not form a rigid and periodic lattice structure. This allows amorphous solids to be more conformationally flexible than crystalline solids, whose rigidity can damage some of the embedded biologics. Amorphous solids are also generally more soluble than their crystalline counterparts which makes rehydration easier and makes them more biocompatible.<sup>17</sup> Anhydrous preservation is modeled after a process that occurs in nature called anhydrobiosis. During anhydrobiosis an organism goes into a dehydrated state in which the organism does not show any signs of life at the metabolic level. However they retain the ability to resume life after rehydration.<sup>18</sup> Tardigrades, also known as water bears, use this technique to survive during times of

extreme dehydration, and can revive themselves once rehydrated.<sup>19</sup> When organisms like the tardigrade are exposed to dehydrated conditions they can produce a disaccharide sugar called trehalose which forms an amorphous solid around the organism to protect the organelles (see Figure 1.1).<sup>20</sup>

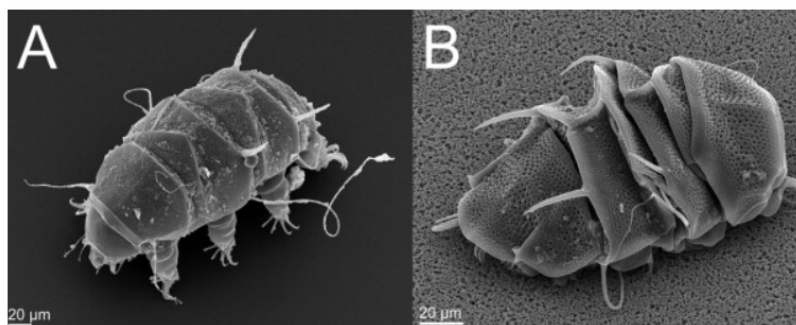


Figure 1.1: Scanning electron micrograph of a tardigrade in (A) its active state and (B) its desiccated state.<sup>20</sup>

The most common techniques for achieving anhydrous preservation for pharmaceutical purposes can be categorized according to their respective transformation mechanism.<sup>21</sup> The first technique involves the direct conversion of a crystalline solid to an amorphous solid, such as milling. The milling process is done by mechanically grinding crystalline solids into a fine powder using rotating mechanical grinders or high velocity air flow.<sup>22</sup> The problem with this method is that mechanical activation methods may not completely disrupt the crystalline structure of the material or can cause a non-uniform distribution of amorphous states resulting in a large range of storage temperatures for the bulk material.<sup>23</sup>

The second technique involves taking a solution and rapidly precipitating the amorphous solid from the solution. The two most common techniques that follow this method are freeze drying and spray drying. Freeze drying is the technique that is most widely used in industry to attempt to stabilize proteins and other biologics. During the freeze drying process, first the protein solution is frozen then the frozen water and the non-frozen bound water are removed from the sample under vacuum.

This process can expose the biologics to extreme temperatures and pressures, which makes it difficult to use with more sensitive biologics. While freeze drying is currently considered the gold standard of protein stabilization, spray drying is another method that is used in some areas to try to rapidly create an amorphous solid from a solution. Spray drying produces a dehydrated powder by atomizing a liquid into a drying environment, resulting in the rapid precipitation of amorphous solids.<sup>24</sup> The drying environment is a closed system containing heated, dry, inert gases. The issue with spray drying is that it can expose the biologics to high temperatures ( $>100^{\circ}\text{C}$ ) and pressures that can be damaging to sensitive biological materials. Further, spray drying exposes the biologics to aseptic conditions making this method difficult to integrate into production lines that produce sterile products. These issues pose a significant challenge for the industrial-scale use of spray drying as a preservation technique.<sup>18</sup>

Of these two general preparation methods for anhydrous preservation, the LAD process utilizes the second technique and involves creating an amorphous solid through rapid precipitation from a solution. Unlike spray drying and freeze drying, the LAD process does not expose the biologic to extreme temperatures or pressures. The LAD process uses an infrared laser to dry bulk droplets of the solution which allows the temperature of the sample during processing to be precisely controlled and also removes any issues that may arise from the high pressures created during the spray drying atomization process. As water is removed from the sample via the LAD process the viscosity of the solution will gradually increase. As long as the solution is not allowed to crystallize, then the viscosity of the solution will eventually become large enough so that the solution will form an amorphous solid. All three of these techniques, LAD; freeze drying; and spray drying, all try to remove water in such a way that prohibits crystallization and forms an amorphous solid. LAD is the only technique that has the capability to do this quickly, precisely, and without exposing

the biologic to extreme temperatures or pressures.

Recent research has suggested that anhydrous, or dry state, preservation in a trehalose amorphous solid matrix may be an alternative to freeze drying and spray drying for the preservation of biological samples.<sup>19,25,26</sup> While freeze drying and spray drying are both considered anhydrous preservation techniques, their methods of water removal are different and so they do not utilize trehalose as a protecting agent. Currently there are four accepted hypotheses for how trehalose protects proteins and other biologics when in an amorphous state. The water replacement hypothesis proposes that trehalose stabilizes a protein by directly interacting with it through hydrogen bonds. Figure 1.2 shows the difference between a protein stabilized through hydrogen bonds during desiccation and a protein that is not stabilized during desiccation. The

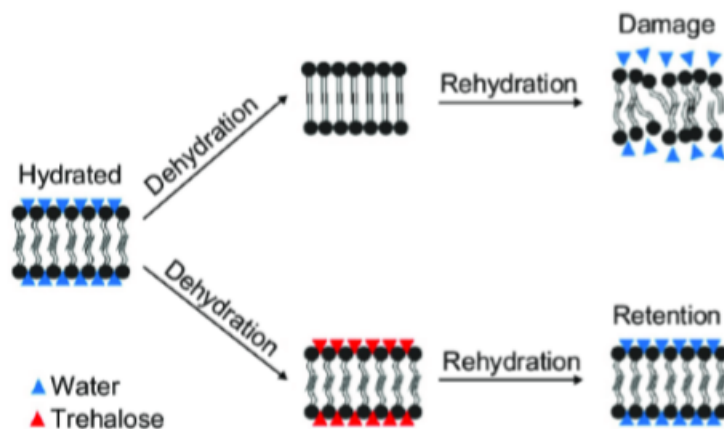


Figure 1.2: A comparison between a protein stabilized through hydrogen bonds (bottom path) and a non-protected protein (top path) during desiccation.<sup>27</sup>

water entrapment hypothesis states that trehalose traps water at the interface of the protein by glass formation, preserving the native solution and thus preserving the protein itself.<sup>28</sup> The mechanical entrapment hypothesis suggests that stabilization occurs by entrapment of the biomolecule in a glass like matrix. This should protect the native conformation of biomolecules like insects trapped in amber. Figure 1.3 shows a protein, lysozyme, encased in an amorphous trehalose matrix. Both the wa-

ter replacement and the water entrapment hypotheses are supported by different sets of experimental and theoretical data.<sup>29-31</sup> The broken glass hypothesis can be thought of as a combination of the water replacement and the water entrapment hypotheses. It suggests the formation of non-uniform patches of trehalose interacting with the protein at specific places that help keep the protein immobile and preserve its higher order structures.<sup>28</sup> Figure 1.4 shows a theoretical model of how this process would look. Which method of preservation is the correct method is still up for debate, as there is evidence supporting all four.

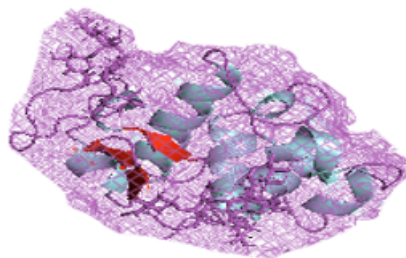


Figure 1.3: A pictorial representation of the mechanical entrapment hypothesis. The trehalose (purple) is completely surrounding the protein (grey and red).<sup>28</sup>

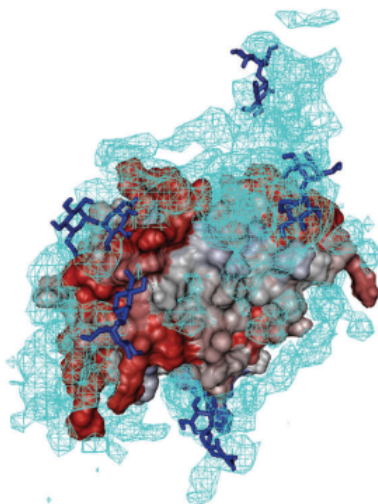


Figure 1.4: Theoretical representation of what the broken glass hypothesis would look like. The trehalose (light blue) is preferentially binding at specific parts of the protein. A few trehalose molecules (dark blue) are shown for size comparison.<sup>28</sup>

Even though the method of preservation is not fully understood, amorphous solids

made of trehalose must obey specific criteria in order to remain in the amorphous state. A trehalose matrix must maintain its amorphous structure to protect an embedded biologic. This can be achieved by storing the sample at or below its glass transition temperature ( $T_g$ ).<sup>32</sup> For an amorphous solid created from a trehalose-water mixture the glass transition temperature can be calculated using the Gordon-Taylor equation,

$$T_g = \frac{x_1 T_{g,1} + k_{gt}(1 - x_1) T_{g,2}}{x_1 + k_{gt}(1 - x_1)}, \quad (1.1)$$

where  $x_1$  is the weight fraction of trehalose,  $T_{g,1}$  is the glass transition temperature of pure trehalose,  $T_{g,2}$  is the glass transition temperature of pure water, and  $k_{gt}$  is an empirically determined fitting parameter.<sup>33</sup> The glass transition temperature for an amorphous trehalose solid formed by dehydration depends on the end moisture content (EMC) of the sample after processing (see Figure 1.5). The EMC of a sample is the ratio of the amount of water left in the sample to the amount of dry weight of the sample. Samples with higher EMC's have higher water content and thus have a lower glass transition temperature. In order for an amorphous solid consisting of trehalose to be stored at room temperature or higher, the sample must have a very low EMC. Achieving a low EMC, while also maintaining the protein or other biologics functionality, is a challenge for anhydrous preservation methods.

### 1.3 This Study

In previous studies LAD has been used to process small volume (10-50  $\mu\text{L}$ ) samples.<sup>15,16,35</sup> In this study, LAD is used to process sample volumes (250  $\mu\text{L}$ ) that are closer to those used for doses of vaccines and therapeutics. Larger volume samples containing the model protein lysozyme were LAD processed and then stored for 1 month in a refrigerator (4°C) and at room temperature (20°C). Thermal histories of the samples during the drying process are used to determine optimal drying parameters and polarized light imaging (PLI) was used to assess the quality of the trehalose

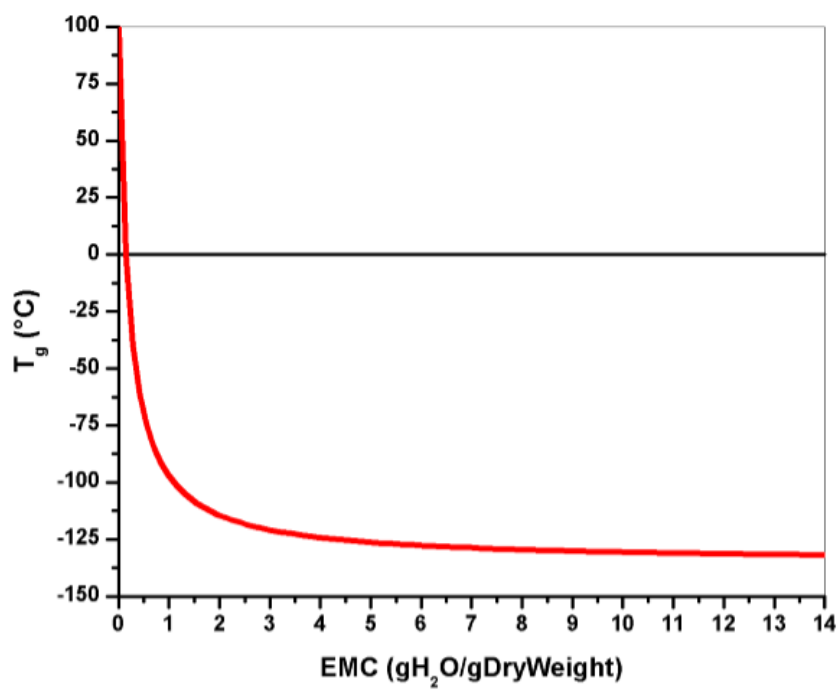


Figure 1.5: Dependence of glass transition temperature of a trehalose-water mixture on end moisture content of the sample, adapted from the Gordon-Taylor equation for binary solutions of polymers.<sup>34</sup>

matrix before and after storage. Raman spectroscopy was used to determine if the water content was equally distributed throughout the samples. Karl-Fischer (KF) Titration was used to measure the water content of LAD processed samples. The results indicate that LAD can successfully stabilize large volume samples for storage at 4°C and at room temperature. A few samples (N=3) stored at room temperature did experience some degradation during storage. This may have been the result of fluctuations in storage temperature.

## CHAPTER 2: METHODS

### 2.1 LAD Processing

A schematic of the LAD processing system is shown in Figure 2.1. An IPG Photonics continuous wave (CW) ytterbium fiber laser at 1064 nm (YLR-5-1064) was used for LAD processing (maximum power output of 5 W). The laser has a factory collimated Gaussian beam with a FWHM spot size of 5 mm which was measured using a BeamTrack 10A-PPS thermal sensor (Ophir Photonics). A FLIR A6 series mid-IR camera was used to record the temperature of samples during processing. All studies were performed in a humidity-controlled environment that was kept at approximately 2% RH. This was achieved by pumping dry air into a chamber containing the experimental setup and monitoring the RH with a temperature and RH logger (ONSET UX100-011). Maintaining a low relative humidity expedited the drying process.

Samples consisted of 250  $\mu\text{L}$  droplets of lysozyme (concentration 0.50 mg/mL) suspended in a drying solution (DS). The DS consisted of 0.2M disaccharide trehalose in 0.33 x phosphate buffer solution (PBS). For each test, a 250  $\mu\text{L}$  droplet of the lysozyme/drying solution was deposited onto an 25 mm diameter borosilicate glass coverslip (Fisherbrand 12-5462) substrate. The diameter of the droplet was approximately 15mm and the thickness was approximately 3mm. These values could vary slightly based on how much the droplet spread out during deposition. The glass coverslips allow for easy recovery and rehydration of the samples after LAD processing. The initial mass of the sample was determined gravimetrically using a 0.01 mg readability balance (RADWAG AS 82/220.R2). The sample was then moved into the humidity chamber for laser irradiation. The samples ( $N = 65$ ) were LAD processed for 2 hours and 20 minutes. The temperature of the sample was monitored during

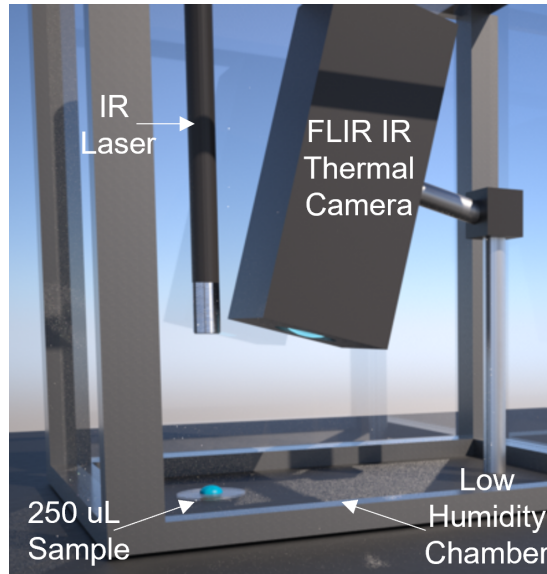


Figure 2.1: LAD experimental set-up within a controlled low relative humidity chamber. A sample is illuminated with a near-IR laser. The temperature of the sample is monitored during processing using the thermal camera.<sup>15</sup>

processing using the thermal camera. The maximum temperature reached during processing was  $42 \pm 1$  °C. After irradiation, the sample was removed from the humidity chamber and immediately massed again. End moisture content (EMC), which is a measure of the amount of water relative to the dry mass of a sample was calculated using Equation 2.1

$$EMC = \frac{m_f - m_s - m_{dw}}{m_{dw}}, \quad (2.1)$$

where  $m_f$  is the mass of the final sample including the mass of the substrate,  $m_s$  is the mass of the substrate, and  $m_{dw}$  is the measured dry weight of the initial sample. After LAD processing, samples were stored individually in small volume containers inside moisture barrier bags (ULine) for 1 month. The RH inside the bags was  $2.0 \pm 0.5$  RH (measured with a RH probe, HH314A, Omega). Samples were stored at 4°C (N=26) and at room temperature (approximately 20°C, N = 30).

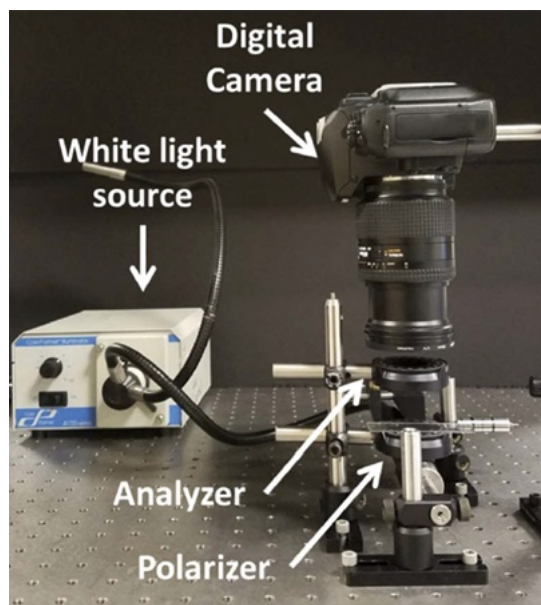


Figure 2.2: Polarized light imaging setup. Samples were placed on a borosilicate glass coverslip between the polarizer and analyzer then imaged from above.<sup>16</sup>

## 2.2 Polarized Light Imaging

To investigate crystal growth in the stored samples, polarized light imaging (PLI) was used. The PLI experimental set-up (Figure 2.2) consisted of a white light fiber optic illuminator (41720, Cole Palmer), two linear polarizers (LPVISE050-A, Thorlabs), with the second polarizer acting as an analyzer, and a digital camera (Nikon D100) aligned in the vertical direction. The camera was equipped with a Nikon 28-105 mm f/3.5-4.5 lens and manually focused on the image plane. The spatial resolution of the set-up was  $10 \mu\text{m}/\text{pixel}$ . Immediately after processing, samples were placed on a glass microscope slide between the polarizers and imaged from above. Two images were taken: the first with the analyzer oriented at  $0^\circ$  to the polarizer and the second with the analyzer oriented at  $90^\circ$  with respect to the polarizer. For each sample, images were taken immediately after processing and after storage.

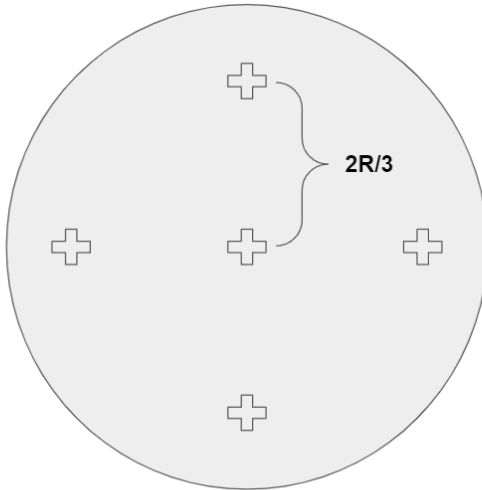


Figure 2.3: Representative image showing the five locations where the Raman spectrum was obtained for each sample.  $R$  is the radius of the sample. The average radius of the samples tested was 7.5mm.

### 2.3 Raman Spectroscopy

To investigate the uniformity of the water content of the samples, Raman spectroscopy was used. Raman spectroscopy was performed on a total of 15 samples. Of those samples, five samples were stored for one month at 4°C, five samples were stored for one month at room temperature, and five samples were tested immediately after LAD processing. A Horiba LabRAM HR800 confocal microscope setup with a 1200 g/mm grating and 532 nm excitation laser wavelength was used to gather the Raman spectra of the samples. Absorption spectroscopy was performed on the solution which showed that the absorption by trehalose and lysozyme is negligible at this wavelength, so there should not be any significant heating of the sample. The 100x (NA = 0.9) objective was used resulting in a spot size of 0.72  $\mu\text{m}$  with a laser power of 11 mW. An integration time of 10 seconds (with 3 accumulations) was used to obtain all spectra. Raman spectra were acquired in five locations at a depth of 20  $\mu\text{m}$  (See Figure 2.3) to sample the spatial distribution of water in the samples.

## 2.4 Karl Fischer Titration

KF Titration is a common titration method that is used to calculate the amount of water present in a sample. KF titration works by adding iodine to a solvent containing the sample being tested. A chemical reaction occurs between the iodine and water in the sample and creates sulfur trioxide and hydroiodic acid. This continues until a small amount of iodine remains present signifying that there is no longer any water left to cause a reaction. The amount of titrant consumed is directly related to the molar amount of water that was present in the sample. Three samples were tested using KF titration. One was tested immediately after LAD processing, one was tested after 5 weeks of storage at room temperature, and one was tested after 5 weeks of storage at 4°C. The sample testing was conducted by Centricor Analytical Labs using their titration system.

## CHAPTER 3: Results and Analysis

### 3.1 End Moisture Contents

A summary of the average EMC of samples immediately after LAD processing, after storage at room temperature, and after storage at 4°C can be seen in Table 3.1. The average EMC of all samples ( $N = 65$ ) after processing for 140 minutes was  $0.20 \pm 0.03$  gH<sub>2</sub>O/gDryWeight. This includes all samples tested during the time of this project, including those that were not stored afterwards. The small standard deviation indicates that the LAD process yields repeatable drying.

Immediately after LAD processing and before storage the average EMC of the samples that were eventually stored at 4°C ( $N = 26$ ) was  $0.21 \pm 0.03$  gH<sub>2</sub>O/gDryWeight. After these samples were stored for one month at 4°C the EMC of the samples was  $0.15 \pm 0.03$  gH<sub>2</sub>O/gDryWeight. On average the EMC of the samples decreased by  $0.06 \pm 0.03$  gH<sub>2</sub>O/gDryWeight during storage. The same trend can be seen with samples that were stored for one month at room temperature ( $N = 30$ ). The samples had an average EMC of  $0.21 \pm 0.02$  gH<sub>2</sub>O/gDryWeight immediately after LAD processing and an average EMC of  $0.12 \pm 0.02$  gH<sub>2</sub>O/gDryWeight after storage. The average change in EMC during storage was  $0.08 \pm 0.02$  gH<sub>2</sub>O/gDryWeight. This is a larger change than for the samples that were stored at 4°C.

Table 3.1: A summary of the average EMC of samples immediately after LAD processing, after storage at room temperature, and after storage at 4° C. Includes the change in EMC before and after storage. All values measured in gH<sub>2</sub>O/gDryWeight.

Sample Type	EMC Before	EMC After	Average Change
All Samples	$0.20 \pm 0.03$	-	-
Stored at 4° C	$0.21 \pm 0.03$	$0.15 \pm 0.03$	$0.06 \pm 0.03$
Stored at Room Temp.	$0.21 \pm 0.02$	$0.12 \pm 0.02$	$0.08 \pm 0.02$

For samples stored at 4°C and samples stored at room temperature, the EMC decreased during storage. An Analysis of Variance (ANOVA) test was performed to determine if the differences between the EMCs before and after storage were statistically significant. An ANOVA test compares the means of two or more independent groups using an F-distribution. The ANOVA test reveals if there is a statistically significant variation between the groups, but it does not indicate which of these groups are different from each other. A post-hoc analysis must be completed to determine between which groups the variation occurs. An ANOVA test was performed on three groups: the EMCs of all samples immediately after LAD processing, the EMCs of samples after storage at 4°C and the EMCs of samples after room temperature storage. The results of the ANOVA test can be seen in Table 3.2. The calculated F-value (106.60) was much greater than the calculated F-crit value (3.10) and the calculated P-value (1.42E-24) was much less than the alpha value chosen for this test (0.05). This means that the null hypothesis can be rejected and that there is a significant statistical variation between two or more of the groups. A Tukey-Kramer post-hoc analysis was performed to determine which of the three group means differed from each other. The Tukey-Kramer test looks at the studentized range distribution of the data to determine which means are different. The results are summarized in Table 3.3. The calculated q-value for all three groups was greater than the calculated q-crit value. This means that there was a statistically significant difference between all three groups. The difference in EMC values reported in Table 3.1 is not due to random error.

The difference in EMC for samples immediately after processing versus after storage demonstrates that evaporation continues during storage further decreasing the EMC. As the EMC of the sample decreases during storage the glass transition temperature increases. This indicates that when samples are stored in a low humidity environment after processing that the appropriate storage temperature will increase as long as the

Table 3.2: A summary of the ANOVA test results for the EMC data.

ANOVA Test Results	F-value	Fcrit-value	P-value
	106.60	3.10	1.42E-24

Table 3.3: A summary of the Tukey-Kramer test results for the EMC data.

Tukey-Kramer Test Groups	q-value	qcrit-value	Difference
Before Storage vs. Room Temperature Storage	19.78	3.37	YES
Before Storage vs. 4° C Storage	12.14	3.37	YES
Room Temperature Storage vs. 4° C Storage	5.62	3.37	YES

initial storage temperature was below the initial glass transition temperature. There is also a difference between the samples that were stored at 4° C versus the samples that were stored at room temperature. This is likely due to the increased evaporation rate of water in samples stored at the higher room temperature.

### 3.2 Thermal Histories

Figure 3.1 shows the thermal histories of all samples that were stored at 4°C (a) and at room temperature (b). These curves show the behavior of the normalized maximum sample temperature as a function of processing time. The normalized maximum temperature was calculated by subtracting the minimum temperature from the maximum temperature. During LAD processing, the ambient room temperature can cause small differences in the maximum temperatures reached during processing. Normalizing the data to the minimum value allows for an easier comparison of the overall shape of the thermal curves. As seen in Figure 3.1, the thermal histories for all samples exhibit the same characteristic behavior. The initial rise in temperature is due to the laser heating the water in the sample. A maximum temperature is then reached within the first 20 minutes. After this peak in temperature, evaporative cooling begins to drive the temperature down. All samples then reach a minimum temperature within 80 minutes of processing. After this the temperature again increases. By the 100 minute mark the amount of heating and evaporative cooling come into an equilibrium and a stabilization of temperature occurs resulting in a plateau in the

thermal curve. This plateau marks the end of significant drying of the sample and is used to help determine the appropriate processing time. Processing further into this region yields little additional drying. In this case, a processing time of 140 minutes ensured that samples reached this plateau.

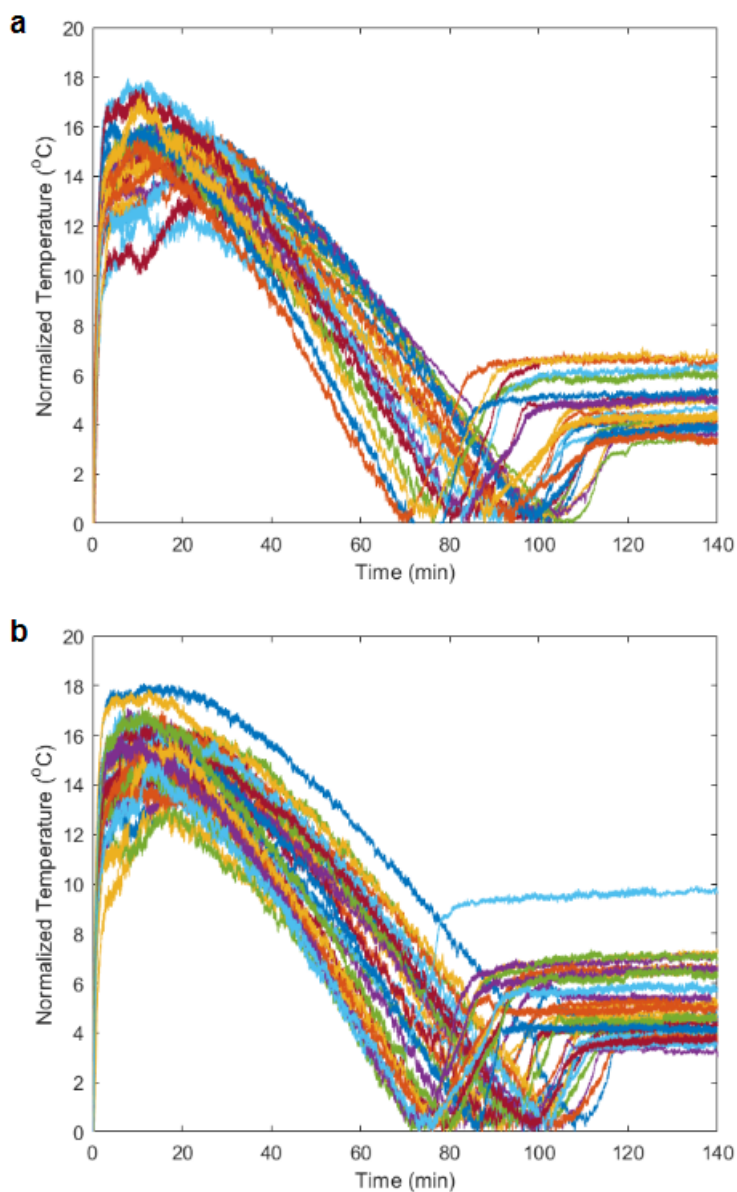


Figure 3.1: Thermal histories for the samples stored at 4°C (a) and room temperature (b).

In order to investigate the dependence of EMC on thermal history, comparisons were made between the thermal histories and the final EMCs of the samples. Figure

3.2 shows EMC vs. the maximum temperature reached by the samples during LAD processing. A Spearman correlation test was done to determine if there was any correlation between the maximum temperature reached and EMC of the sample after processing. The Spearman correlation test is the nonparametric version of the Pearson correlation test and can be used for data with a non-normal distribution. The Spearman coefficient was determined to be 0.29 (see Table 3.4). This falls below the critical alpha value of 0.42 and indicates with greater than 99% certainty that there is little/no correlation between EMC and maximum temperature. This suggests that the final EMC does not depend on the peak temperature reached during processing as long as samples are processed until they reach the temperature plateau.

A similar test was conducted to investigate the dependence of the change in temperature on final EMC. The change in temperature is denoted as the difference between the maximum and minimum temperatures reached during LAD processing. A plot of the data is shown in Figure 3.3. The Spearman coefficient for this data set was -0.16 (see Table 3.4). This value again indicates that there is little/no correlation between EMC and the change in temperature. These results suggest that the final EMC does not depend on the difference between the maximum and the minimum temperature as long as samples are processed until they reach the temperature plateau. This suggests that small changes in ambient temperature do not affect the final EMC of the sample.

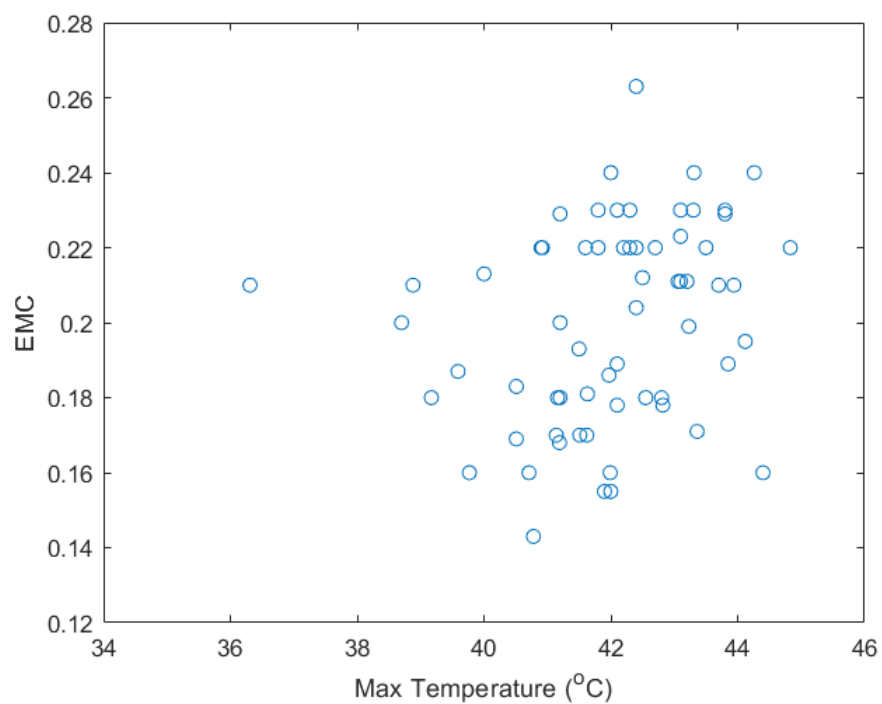


Figure 3.2: EMCs of samples as a function of maximum temperature reached during processing.

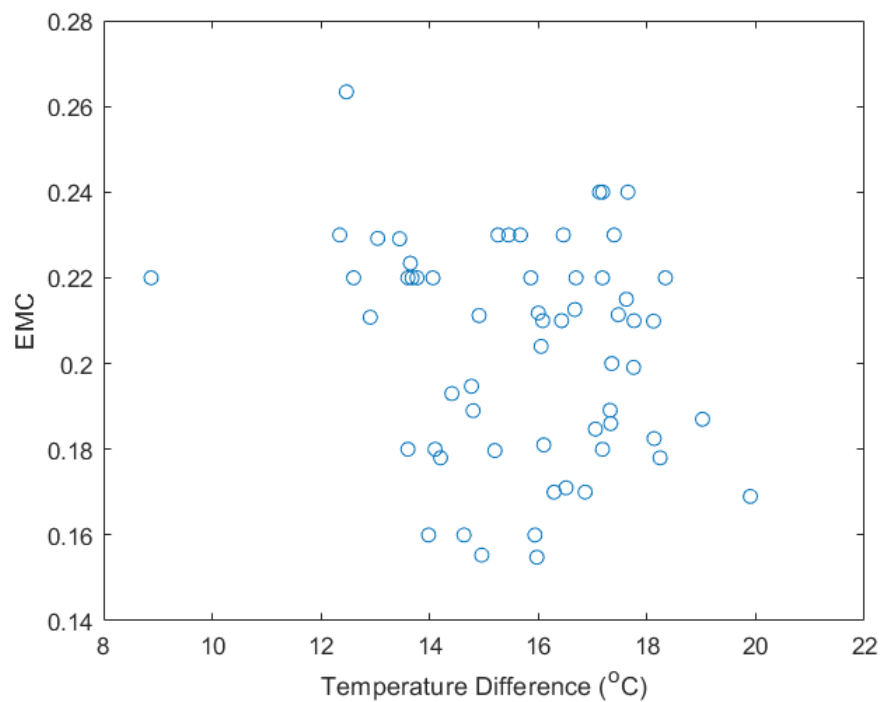


Figure 3.3: EMCs of samples as a function of change in temperature during processing.

Table 3.4: Spearman correlation coefficients between EMC and maximum temperature, and EMC and change in temperature.

Measurement Type	Spearman Coefficient
EMC vs. Max Temperature	0.29
EMC vs Change in Temperature	-0.16

### 3.3 Polarized Light Imaging

Figure 3.4 shows representative polarized light images of a sample taken immediately after LAD processing (a-b) and after 1 month of storage at 4° C (c-d). Figure 3.4a and Figure 3.4c show images taken with the polarizer and analyser at the same angle. Figure 3.4b and Figure 3.4d show crossed-polarizer images. There is little/no crystallization evident in either of these images. This indicates that the LAD processed trehalose matrix was resistant to crystallization during processing and after storage at 4°C.

Figure 3.5 shows representative polarized light images of a fully crystallized sample taken immediately after LAD processing (a-b) and after 1 month of storage (c-d). This sample was stored at room temperature, however, it does not represent all room temperature samples. This sample is shown to highlight how crystallization will look if present in a sample. Figure 3.5a and Figure 3.5c show the images of a sample taken with the polarizer and analyser at the same angle. These images show a detailed view of the sample before and after storage. Figure 3.5b and Figure 3.5d show crossed-polarizer images of the sample. Crystalline inclusions in the sample will rotate the plane of polarization of the incident polarized light making crystallized areas of the sample appear as white spots in the image. For this sample a small amount of crystallization is present immediately after processing and a large amount of crystallization is evident after 1 month of storage at room temperature. When storing samples above their glass transition temperature crystallization can occur. This glass transition temperature is dependent on the water content of the sample -

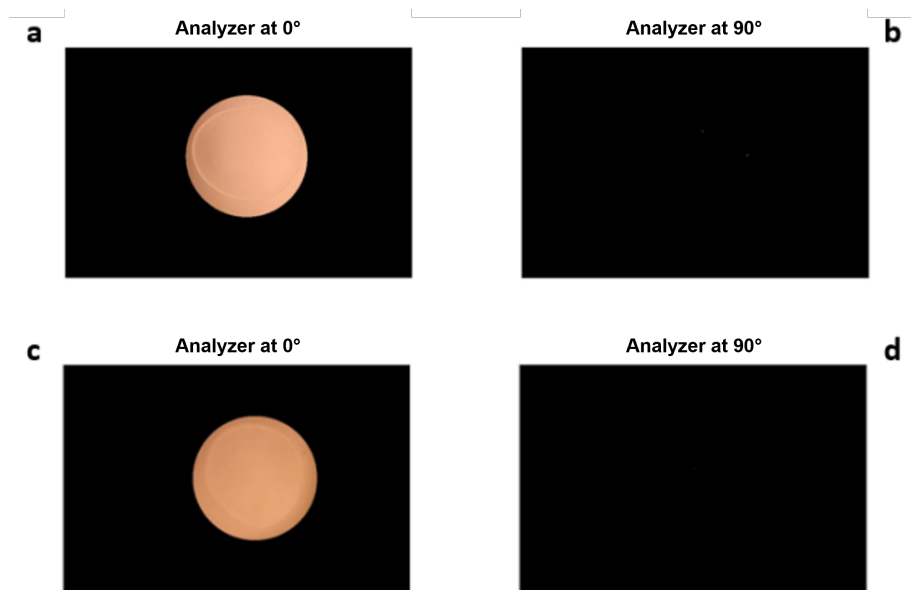


Figure 3.4: PLI of a LAD processed sample where (a-b) were taken immediately after LAD processing and (c-d) were taken after 1 month of storage at 4°C. Images a and c were taken with the polarizer and analyser at the same angle. Images b and d are the crossed-polarizer images and areas of crystallization should appear white in these images.

a low EMC is necessary for storage at higher temperatures. These images indicate that the EMC of this sample was not low enough for the amorphous matrix to remain stable against crystallization at room temperature.

Crystal areas were calculated based on the PLI in MATLAB using a thresholding technique. For each image taken with crossed polarizers, a threshold intensity was established by finding the average maximum value of intensity of an area of pixels outside the sample. All pixels with intensities below the threshold value were zeroed. Crystal area was then measured as the number of pixels with intensity higher than zero in the crossed polarizer image. Table 3.6 summarizes the measured crystal area of LAD processed samples before and after 1 month of storage at room temperature and Table 3.5 summarizes the measured crystal area of LAD processed samples before and after 1 month of storage at 4°C.

Problems with the PLI setup resulted in defocused images for several samples after

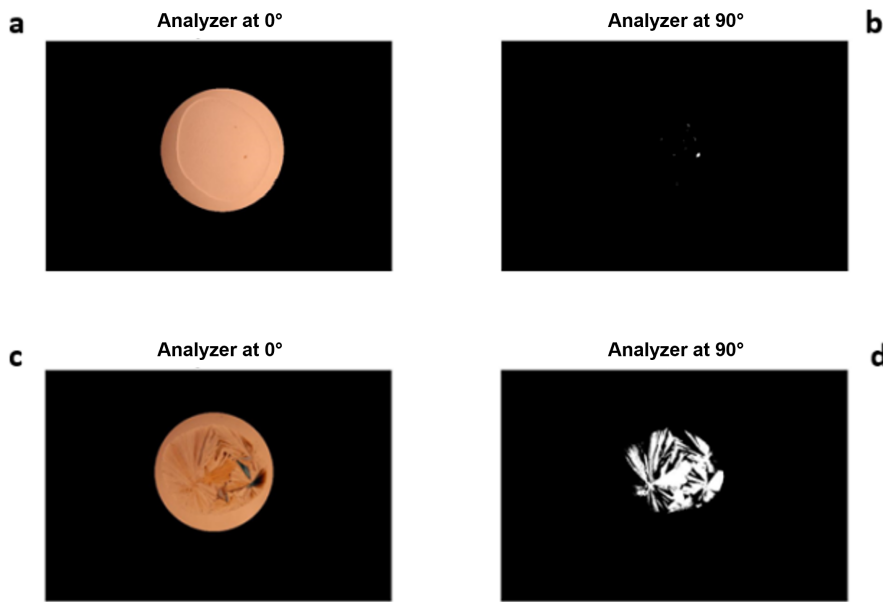


Figure 3.5: PLI of a LAD processed sample where (a-b) were taken immediately after LAD processing and (c-d) were taken after 1 month of storage at room temperature. Images a and c were taken with the polarizer and analyser at the same angle. Images b and d are the crossed-polarizer images and areas of crystallization should appear white in these images.

storage and these samples are not included in the table. Impurities in a sample (dust, etc.) can be measured as a small crystal area in a sample immediately after processing. However, this measured pixel area does not change during storage and does not indicate that a sample is unstable. For this reason, the tables referenced above also list the change in the crystal area before and after storage. This difference is an indication of crystal growth in the samples and large crystal growth is an indication that the matrix has crystallized. For the samples stored at 4°C, 3 out of 24 samples (3,4,5) show a large amount of crystallization after storage. Note however, that these three samples exhibited a relatively high crystal area immediately after processing. The remaining samples showed little to no significant crystal growth during storage. A similar trend is seen for the LAD processed samples stored for 1 month at room temperature. The majority of these samples exhibited little to no significant crystal growth.

In order to determine if the trehalose matrix was truly resistant to crystal formation, an ANOVA test and Tukey-Kramer post-hoc analysis were performed to compare the crystal areas of samples before and after storage. The results of the ANOVA test are shown in Table 3.7. The calculated F-value is larger than the calculated  $F_{crit}$ -value, and the p-value is smaller than the alpha value chosen for this test (0.05) revealing that there is some significant statistical difference between two or more of these groups. The results of the Tukey-Kramer analysis are shown in Table 3.8. The before storage versus room temperature storage group was the only group in which the q-value was greater than the q-crit value. This means that for samples stored at room temperature, there is a statistically significant difference in crystal area present when compared to the before storage samples. It should be noted that two of the room temperature stored samples have a change in crystal area that is more than three times larger than that of the next highest sample (samples 2 and 3 in Table 3.6). The crystallization seen in these samples could be due to fluctuations in room temperature during storage as they were not stored in a controlled environment. If an ANOVA test excludes these two outliers then the F-value falls below the  $F_{crit}$ -value and there is no statistically significant difference present between any of the groups, signaling that in most cases room temperature storage is still resistant to crystal growth while in all instances the fridge storage samples are resistant to crystal growth. This is likely due to the glass transition temperature of the trehalose matrix being close to that of room temperature. Most samples will remain resistant to crystal growth but those with slightly lower glass transition temperatures may be prone to crystallization.

Table 3.5: Crystal growth of samples after 1-month storage at 4°C. Crystal growth is measured in pixels.

Sample Number	Before Storage	After Storage	Change in Crystal Area
1	10	0	10
2	112	1	109
3	1847	67282	65435
4	811	53268	58728
5	855	14759	13909
6	0	0	0
7	0	0	0
8	0	1	1
9	257	285	28
10	134	244	110
11	114	146	32
12	0	24	24
13	205	102	103
14	160	49	111
15	146	103	43
16	15	0	15
17	98	47	51
18	189	101	188
19	131	314	183
20	337	156	181
21	41	839	798
22	34	268	234
23	16	3	13
24	110	153	43

Table 3.6: Crystal growth of samples after 1-month storage at room temperature (20°C). Crystal growth is measured in pixels.

Sample Number	Before Storage	After Storage	Change in Crystal Area
1	32	71734	71767
2	0	177130	178160
3	924	262230	261350
4	2686	71079	68602
5	0	0	0
6	174	583	409
7	107	196	89
8	169	134	35
9	365	474	109
10	18	174	156
11	186	749	563
12	0	0	0
13	40	385	345
14	261	127	134
15	0	0	0
16	385	277	108
17	2	295	293
18	631	869	238
19	0	3	3
20	2	3	1
21	788	557	231
22	166	721	555
23	652	2061	1409
24	556	2588	2032
25	7	2	5
26	69	1935	1866
27	1	0	1
28	3	56	53

Table 3.7: A summary of the ANOVA test results for the PLI data.

ANOVA Test Results	F-value	Fcrit-value	P-value
	3.89	3.09	0.02

Table 3.8: A summary of the Tukey-Kramer test results for the PLI data.

Tukey-Kramer Test Groups	q-value	qcrit-value	Difference
Before Storage vs. Room Temperature Storage	3.93	3.36	YES
Before Storage vs. 4° C Storage	0.98	3.36	NO
Room Temperature Storage vs. 4° C Storage	2.44	3.36	NO

### 3.4 Raman Spectroscopy

Figure 3.6 shows a representative Raman spectrum of a LAD processed sample. Peak 1 occurs near  $850\text{ cm}^{-1}$  and is due to a C-O-C skeletal structure in trehalose. Peak 2 occurs near  $900\text{ cm}^{-1}$  and is due to a C-C stretch in trehalose. Peak 3 occurs near  $3400\text{ cm}^{-1}$  and is due to an O-H stretch feature that has contributions from both trehalose and water.<sup>36</sup> Line intensities for these three peaks were calculated by removing a baseline (determined in the  $3700 - 4000\text{ cm}^{-1}$  region) and integrating under the peaks. Peaks 1 and 2 are both due to trehalose. The intensity ratio of these features should be constant throughout our samples. The intensity ratios of peak 3 to peak 1 (3:1) and peak 3 to peak 2 (3:2) are measures of the relative amount of water in a LAD processed sample. These ratios can be used to study the uniformity of the water distribution in samples after LAD processing.

The 3:1 and 3:2 ratios should be correlated with the water content of a sample (see Table 3.9). To verify that this was indeed the case, the average 3:1 and 3:2 ratios were calculated for each droplet and a Spearman correlation test was performed between the EMC of a sample and the mean value of the 3:1 and 3:2 peak ratios. For both ratios, the Spearman coefficient was above the alpha value. This suggests that the mean value of the 3:1 and 3:2 peak ratios are in fact correlated with water content. The larger the ratio, the higher the water content.

How the values of the 3:1 and 3:2 peak ratios are related across the groups (no storage,  $4^\circ\text{ C}$  storage, room temperature storage) provides insights into how the water content of a sample changes during storage. An ANOVA test was used to compare the mean values of the 3:1 and 3:2 peak ratios of samples across the three groups. The results are shown in Table 3.10. For the 3:1 and 3:2 peak ratios the calculated F-value was larger than the calculated  $F_{\text{crit}}$ -value and the p-value was smaller than the alpha value chosen for this test (0.05). This shows that there is some variation in the mean values of the 3:1 and 3:2 peak ratios as a function of storage type. A

Table 3.9: EMCs and Average Line Ratios for All Samples. The EMC is given in units of  $\text{gH}_2\text{O/gDryWeight}$ .

	EMC	Average 3:1 Ratio	Average 3:2 Ratio
No Storage			
Sample a	0.22	24.80	26.52
Sample b	0.17	26.15	30.87
Sample c	0.17	26.46	31.72
Sample d	0.16	24.68	29.12
Sample e	0.14	26.23	31.02
4°C Storage			
Sample a	0.19	23.86	28.02
Sample b	0.19	25.74	30.44
Sample c	0.17	24.37	28.54
Sample d	0.16	22.23	25.92
Sample e	0.14	22.16	25.74
Room Temperature Storage			
Sample a	0.18	25.38	29.79
Sample b	0.15	22.21	25.87
Sample c	0.14	21.98	25.52
Sample d	0.13	22.21	25.58
Sample e	0.13	21.72	25.20

Tukey-Kramer post-hoc analysis was performed for both peak ratios and the results are shown in Table 3.11 and Table 3.12 respectively. There is variation in the mean values of the 3:1 peak and 3:2 ratios between the no storage samples and the room temperature storage samples. This means that the amount of water present in the samples before and after room temperature storage is statistically different. This agrees with the previous finding that the average EMC of samples stored for one month at room temperature was lower than the average EMC of samples immediately after processing. Drying continued during storage.

Table 3.10: A summary of the ANOVA test results for the mean values of the 3:1 and 3:2 peak ratios.

Peak Ratio	F-value	Fcrit-value	P-value
3:1	6.44	3.89	0.01
3:2	4.11	3.89	0.04

Table 3.11: A summary of the Tukey-Kramer test results for the mean values of the 3:1 peak ratios.

Tukey-Kramer Test Groups	q-value	qcrit-value	Difference
Before Storage vs. Room Temperature Storage	4.98	3.77	YES
Before Storage vs. Fridge Storage	3.34	3.77	NO
Room Temperature Storage vs. Fridge Storage	1.63	3.77	NO

Table 3.12: A summary of the Tukey-Kramer test results for the mean values of the 3:2 peak ratios.

Tukey-Kramer Test Groups	q-value	qcrit-value	Difference
Before Storage vs. Room Temperature Storage	4.02	3.77	YES
Before Storage vs. Fridge Storage	2.48	3.77	NO
Room Temperature Storage vs. Fridge Storage	1.53	3.77	NO

Figure 3.7 shows the 2:1 and 3:1 peak intensity ratios as a function of position within LAD processed samples. Images a-e each represent an individual sample. These samples were not stored and Raman spectroscopy was completed immediately after LAD processing. Position 3 is at the center of the sample and positions 1, 2, 4, and 5 are located at two thirds of the radius away from the center (see Figure 2.3). The measured EMC of each sample is shown at the top of each graph. Figure 3.8 shows the 2 to 1 and 3 to 1 peak intensity ratios as a function of position for samples that were stored for one month at 4°C and Figure 3.9 shows these peak intensity

ratios for samples that were stored for one month at room temperature. The 3:2 ratios are not shown but show a similar trend. The only difference is a scaling factor that can be directly related to the value of the 2:1 ratio.

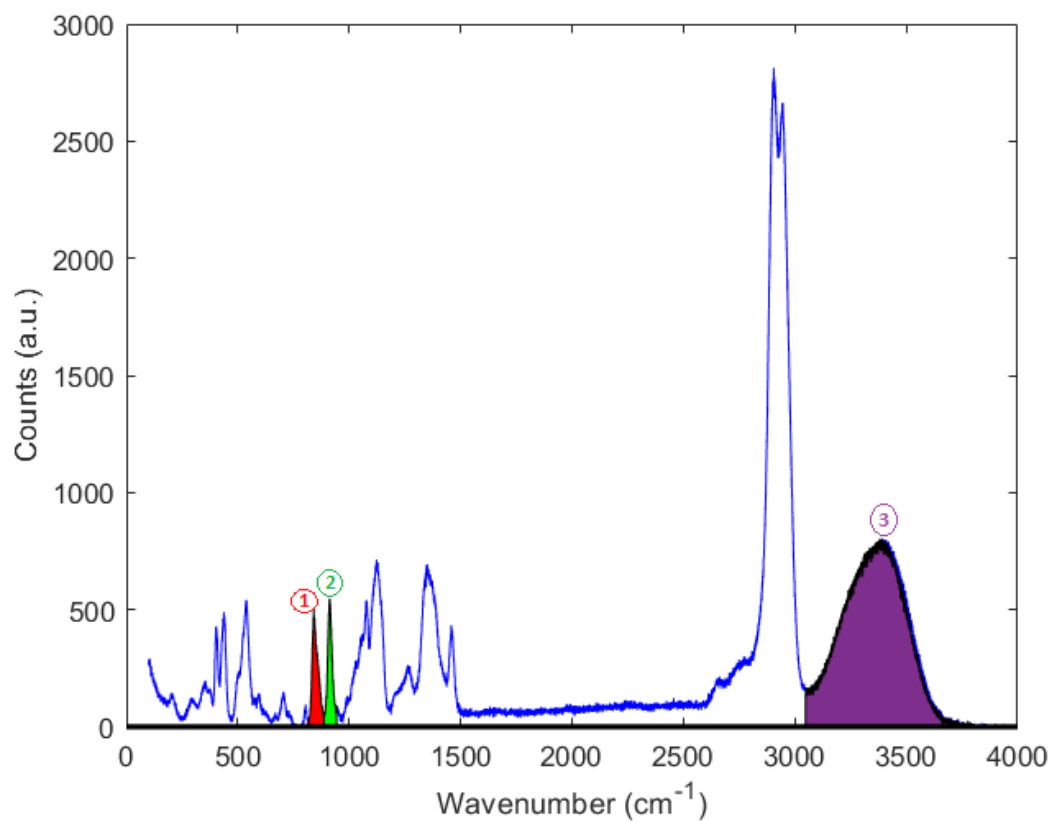


Figure 3.6: Representative Raman spectrum for a LAD processed sample. Peaks 1 and 2 are due to trehalose and peak 3 contains contributions from both water and trehalose.

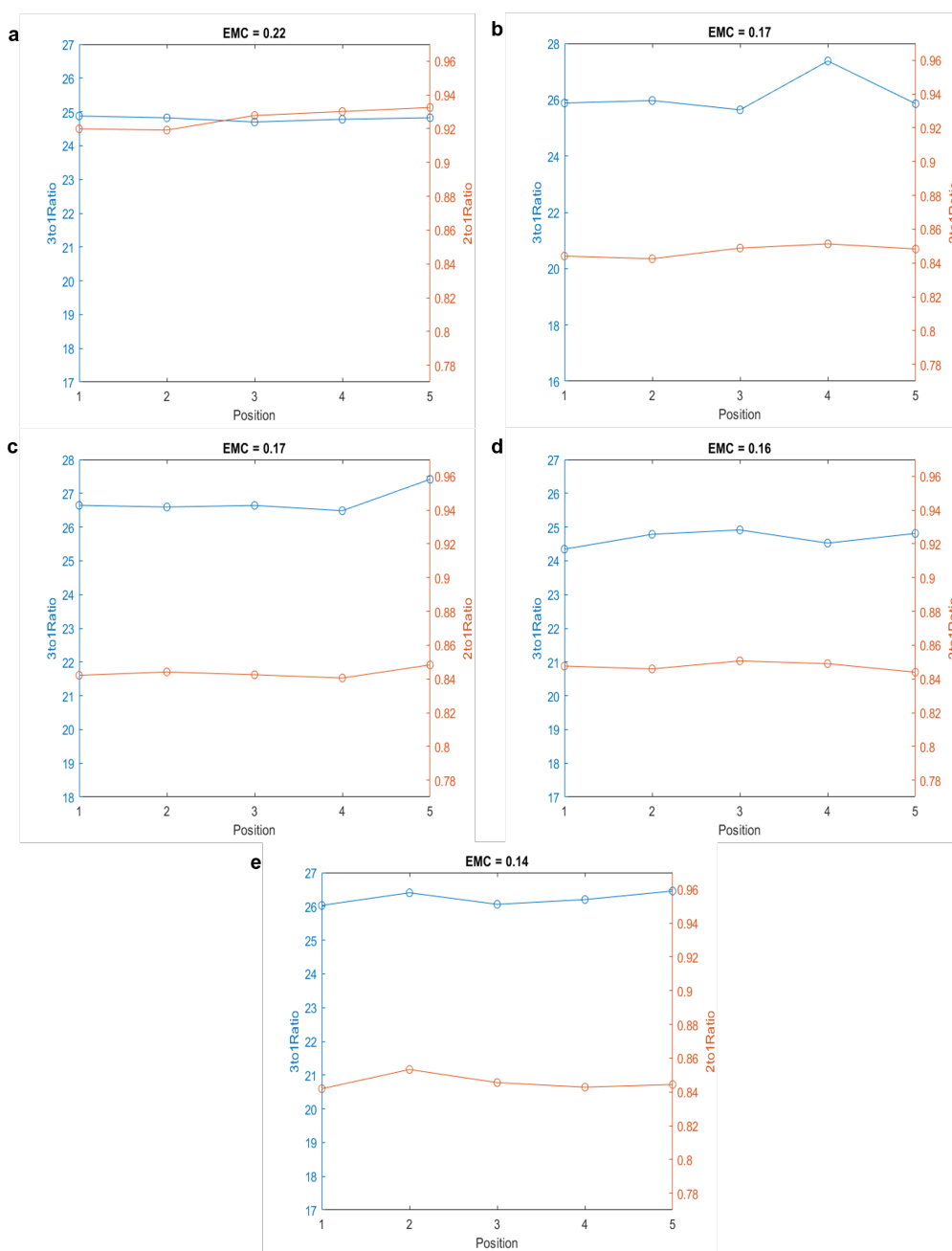


Figure 3.7: Line ratios as a function of position for LAD processed samples. These samples were not stored and Raman spectroscopy was performed immediately after LAD processing. The 3to1Ratio axis represents the water to trehalose comparison and the 2to1Ratio axis represents the trehalose to trehalose comparison.

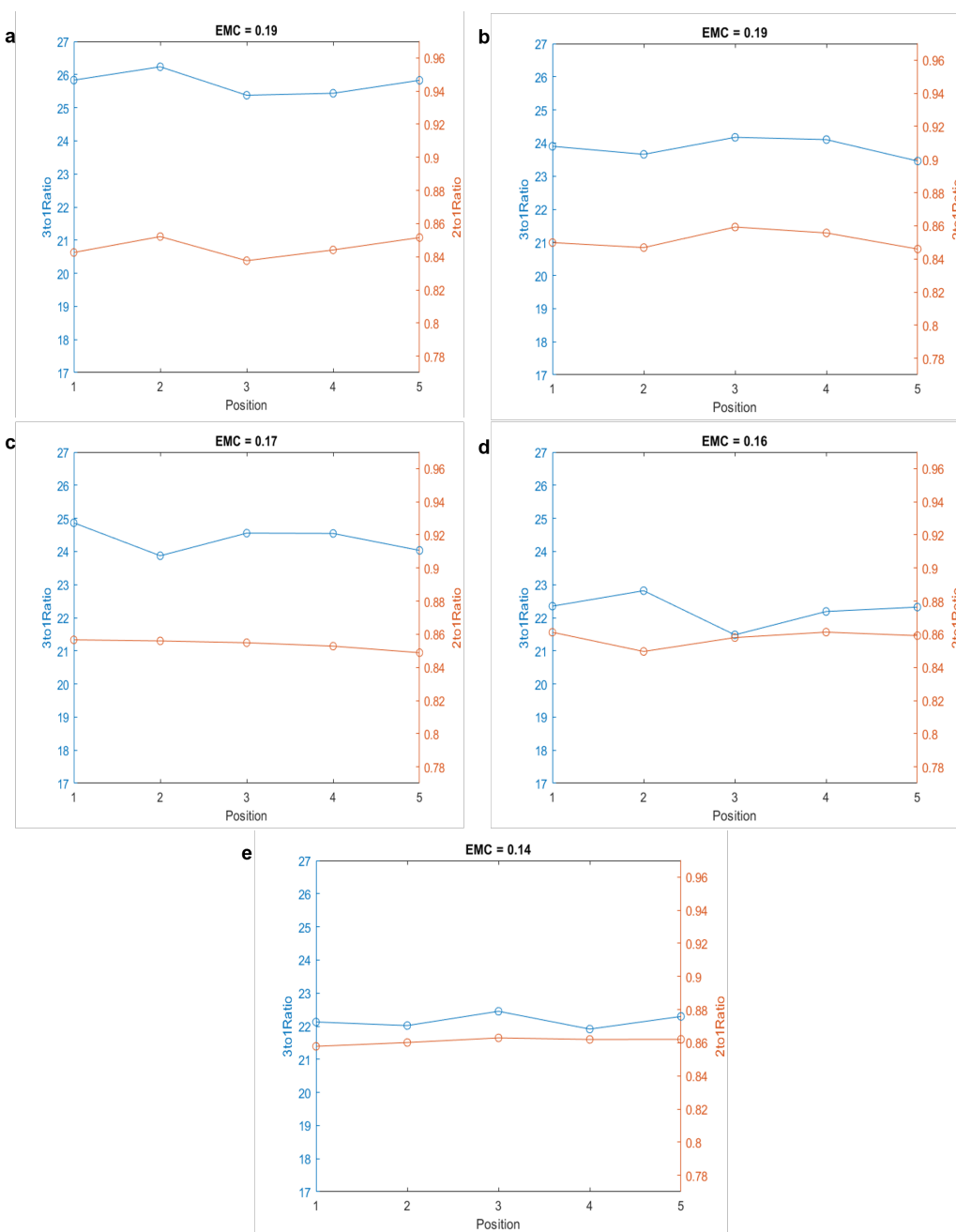


Figure 3.8: Line ratios as a function of position for LAD processed samples stored for one month at 4°C. The 3to1Ratio axis represents the water to trehalose comparison and the 2to1Ratio axis represents the trehalose to trehalose comparison.

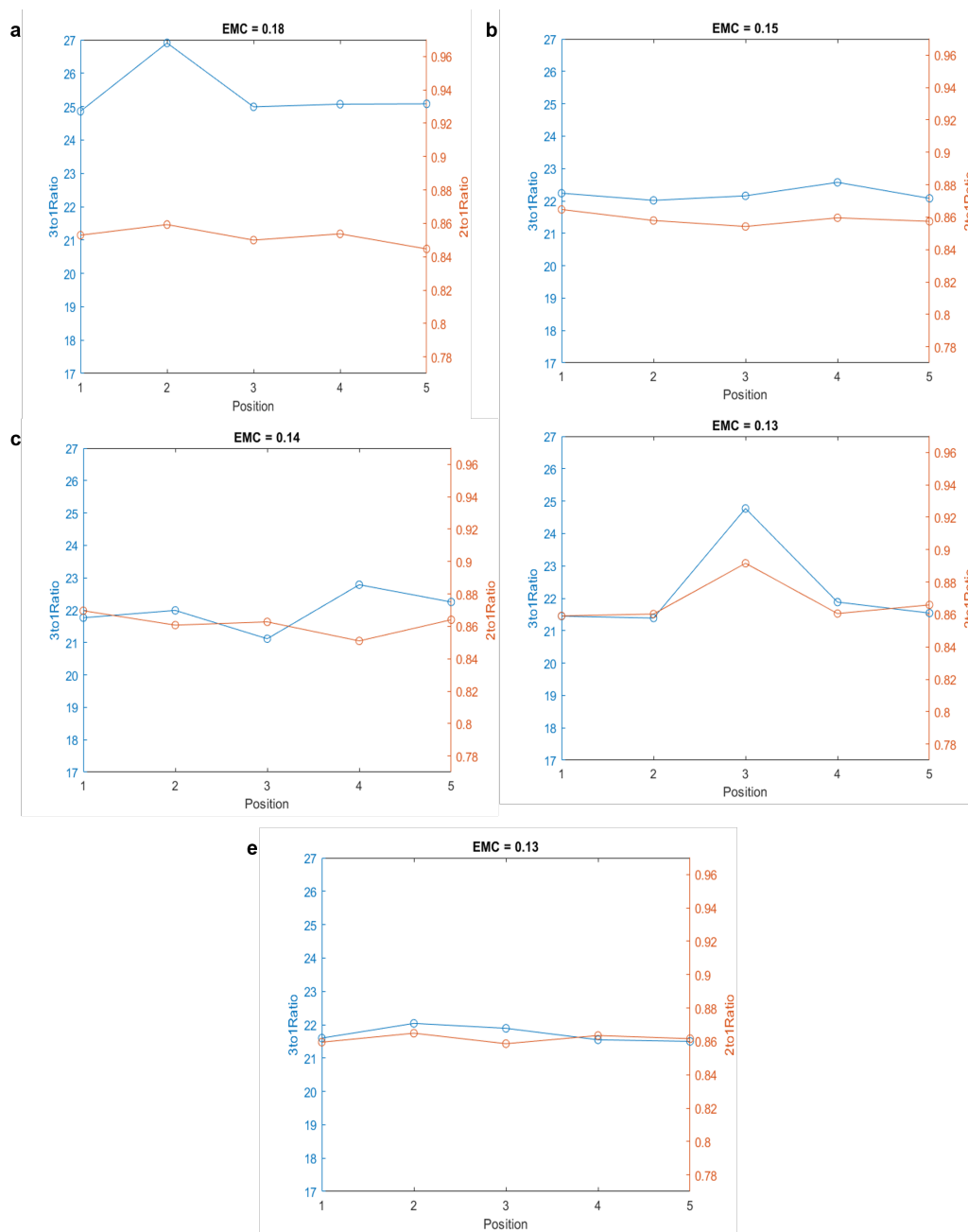


Figure 3.9: Line ratios as a function of position for LAD processed samples stored for one month at room temperature. The 3to1Ratio axis represents the water to trehalose comparison and the 2to1Ratio axis represents the trehalose to trehalose comparison.

To quantify the variation of the 2:1, 3:1 and 3:2 ratios as a function of position within individual samples, the coefficient of variation (COV) was calculated. The COV reveals how much individual measurements within a data set vary relative to the mean of the data. The COV for each sample is shown in Table 3.13. The COV for the 2:1 ratio is less than 1% for all but one sample suggesting that the trehalose distribution is consistent throughout each sample. The COV values for the 3:1 and 3:2 ratios are slightly larger than for the trehalose suggesting a small variation in the water content as a function of position. However, this variation is less than 6.5% for all of samples.

The COV analysis indicates that the line ratios only vary by a small amount across the droplets. To better understand how this variation in the line ratios relates to the variation of the water content, the average EMCs of samples and the average values of the 3:1 and 3:2 ratios were examined (see Table 3.9). The percent difference between the highest and lowest mean peak ratio was calculated across all samples. For the 3:1 ratio, the percent difference between the highest and lowest mean peak value was 19.7%. For the 3:2 ratio the percent difference between the highest and lowest mean peak ratio value was 23.0%. The difference between these two values is directly proportional to the average 2:1 peak ratio value as expected. The EMCs for samples varied from 0.13 to 0.22. These samples did not crystallize, indicating that the water content in all samples was low enough for the trehalose matrix to remain in the amorphous state after processing. Variation in the 3:1 and 3:2 line ratios of approximately 20% does not seem to negatively affect the integrity of the matrix. The largest COV for our samples was 6.5% and this is well below the 20% threshold percent difference between the highest and lowest mean peak ratio value. This signifies that the LAD process dries samples relatively uniformly, meaning that the variation of the glass transition temperature of the samples as a function of position is negligible for storage at temperatures at or below room temperature. This

is significant because uneven distribution of water would result in an inconsistent glass transition temperature as a function of position. This is not ideal as a difference in this glass transition temperature could lead to crystal seeding and matrix instability while a sample is in storage.

The average COV for the 3:1 and 3:2 was calculated for the three groups (no storage, 4° C storage, room temperature storage) and an ANOVA test was used to determine if there was a difference in the variation of the line ratios across the groups. The ANOVA test revealed that there was no variation in the COV values between the groups, meaning that amount of variation in water content was consistent across the groups. This suggests that the small variation in water content seen in the samples is the result of processing and is not the result of the different storage temperatures.

A Spearman correlation test was performed to determine if there was any correlation between the EMC of a sample and the COV for the 3:1 and 3:2 peak ratios. In both cases the Spearman coefficient was below the alpha value indicating that the COV also remains consistent as a function of EMC. The small spatial variation in water content is not correlated with the EMC of the samples.

### 3.5 Karl Fischer Titration

The water content of three samples was measured using KF Titration. Table 3.14 shows the percent water content by mass of the samples, as well as the EMC of the samples after storage along with the theoretical glass transition temperature. It should be noted that the EMC after processing/storage was calculated directly from the water content (not from the theoretical dry weight). This is why the values are different than other EMCs reported earlier. The calculation from the KF results is more accurate. The EMC based on dry weight is not a good measure of absolute water content, but instead can be used to quantify the relative water content between samples. The glass transition temperature was calculated using the Gordon-Taylor equation for a binary solution of water and trehalose.<sup>34</sup> This equation does not include

Table 3.13: The COV as a function of position for the 2:1, 3:1 and 3:2 line ratios for all samples. The EMC of the sample at the time of testing is given in units of gH<sub>2</sub>O/gDryWeight.

	EMC	3:1 COV	3:2 COV	2:1 COV
No Storage				
Sample a	0.22	0.27 %	0.81 %	0.65 %
Sample b	0.17	2.7 %	2.5 %	0.43 %
Sample c	0.17	1.4 %	1.1 %	0.35 %
Sample d	0.16	0.95 %	1.0 %	0.31 %
Sample e	0.14	0.74 %	0.64 %	0.54 %
4°C Storage				
Sample a	0.19	1.4 %	0.89 %	0.73 %
Sample b	0.19	1.3 %	0.66 %	0.68 %
Sample c	0.17	1.7 %	1.6 %	0.37 %
Sample d	0.16	2.2 %	2.5 %	0.56 %
Sample e	0.14	0.97 %	0.90 %	0.24 %
Room Temperature Storage				
Sample a	0.18	3.4 %	2.9 %	0.63 %
Sample b	0.15	0.98 %	0.94 %	0.45 %
Sample c	0.14	2.8 %	3.4 %	0.79 %
Sample d	0.13	6.5 %	4.9 %	1.6 %
Sample e	0.13	1.1 %	1.1 %	0.31 %

Table 3.14: The water content of samples tested using KF Titration. The EMC is given in gH<sub>2</sub>O/gDryWeight. The theoretical glass transition temperature is given in °C.

Storage Method	Water Content	EMC	T <sub>g</sub>
Same Day	2.0%	0.020	77.5
Room Temperature	2.4%	0.025	73.4
Fridge	0.80%	0.0081	90.5

lysozyme or the salts in the PBS buffer, therefore it is only an estimate of the glass transition temperature.

The sample with the highest water content was the room temperature (approximately 20°C) stored sample. This sample contained 2.4% water. The same day sample had the next highest water content at 2.0%. The sample with the lowest water content was the fridge (4°C) stored sample. This sample contained 0.8% water. These results show that the LAD process is able to effectively remove the majority of the water from a sample. Based on the PLI and Raman results discussed earlier, this also shows that achieving water contents below 2.5% has the potential to yield a uniformly dry trehalose matrix that is resistant to crystallization. The theoretical glass transition temperatures for all samples was above 73°C. This is much higher than the temperatures experienced during room temperature storage (roughly 20°C). This suggests that these LAD processed samples could have tolerated much harsher storage conditions. More investigation is warranted to see if LAD processed samples can truly be stored at these elevated temperatures.

## CHAPTER 4: Discussion and Conclusions

Large volume samples (250  $\mu\text{L}$ ) containing the protein lysozyme were LAD processed for 140 minutes and stored for 1 month at 4°C or room temperature. The average EMC for these large volume samples was  $0.20 \pm 0.03$  gH<sub>2</sub>O/gDryWeight. The low standard deviation indicates that LAD processing results in consistent EMCs and therefore consistent glass transition temperatures. Maintaining consistent glass transition temperatures is important when considering the storage temperature for the transportation of your samples. A low variation in the storage temperature reduces the risk of sample loss with minor temperature fluctuations.

Thermal histories of the samples were taken during processing using a FLIR thermal camera. This allows the temperature of the samples to be monitored without having to physically make contact with the samples. This allows you to more easily maintain a sterile environment. The thermal histories show significant water loss during the first 60-80 minutes of processing. By 140 minutes evaporative water loss has significantly slowed. These curves were used to determine the 140 minute LAD processing time used in this study. A comparison of the maximum temperature reached during LAD processing and the EMC of the sample immediately after processing, as well as a comparison of the change in temperature during processing and the EMC reached immediately after processing was completed. There was no significant correlation between EMC and maximum temperature, and EMC and change in temperature. During processing there can be minor variations in the maximum temperature as well as the change in temperature that the samples experience. This is due to fluctuations in the ambient temperature of the room where processing is occurring. With no correlation being found between EMC and temperature reached during processing this

signifies that the LAD process is not sensitive to small changes in ambient temperature and therefore is highly repeatable.

PLI images that were taken immediately after processing and after 1 month of storage indicate that samples stored at 4°C and at room temperature had little/no crystallization. Crystallization can cause mechanical stresses on the embedded biologic so it is important that during storage the trehalose matrix remains in an amorphous state. These results indicate that the average EMC of the 250  $\mu\text{L}$  samples is low enough to store at room temperature and at 4°C without significant degradation of the trehalose matrix. Considering that most biologics have to be stored at or below freezing, being able to store LAD processed samples at room temperature is already a vast improvement over conventional biopreservation techniques.

Raman spectroscopy was done to investigate the uniformity of the water content of the samples. Raman spectra were acquired in five locations across the droplet and line ratios were calculated to measure the relative amount of water in a LAD processed sample. Results showed that the variation of water distribution across a sample was relatively small, meaning that the samples were uniformly dried and therefore the EMC of the sample does not vary greatly as a function of position within the sample. Further study is required to determine the exact variation of the EMC within a sample. Results also showed that there was a correlation between the average EMC of the sample and the average intensity of the 3:1 and 3:2 peak ratios. This proves that these peak ratios do give information regarding water content. This could also be used in the future as an alternative means to calculating the water content of a sample.

Karl Fischer Titration was done to investigate the true water content of LAD processed samples. Three samples were tested. One was tested the same day it was processed, one was tested after five weeks of storage at room temperature, and one was tested after five weeks of storage in the fridge. All three samples had a water

content below 2.5%. This is comparable to the water content of lyophilized samples. This also proves that the LAD process is able to effectively remove the majority of water from a sample without causing significant crystallization. The theoretical glass transition temperature for all samples was above 73°C. This suggests that LAD processed samples could tolerate much harsher storage conditions. More investigation is warranted to see if LAD processed samples can truly be stored at these elevated temperatures.

For future work, an extended study with KF Titration should be conducted to more effectively gain an understanding of the true water content of LAD processed samples. Results of this study could be used to determine a direct relation between EMC and water content. Once this relation is established, EMC could then be used in place of KF Titration to calculate the true water content of LAD processed samples. Samples should also be stored at higher temperatures during this trial. Further, KF Titration and Raman Spectroscopy should be done on samples with varying EMCs so that a relation can be established between the EMC of a sample and the line ratio values of a sample. This would allow for a true determination of the water content distribution throughout a sample. Moreover, LAD should be tested on more sensitive biologics such as vaccines and at higher volumes equivalent to therapeutic doses. These doses are typically in the range of 500 $\mu$ L to 1000 $\mu$ L. Eventually, LAD will need to be implemented in an industrial setting for large scale use.

## REFERENCES

- [1] Leader, B., Baca, Q. J., and Golan, D. E., "Protein therapeutics: a summary and pharmacological classification," *Nat Rev Drug Discov* **7**(1), 21–39 (2008).
- [2] Kingsmore, S. F., "Multiplexed protein measurement: technologies and applications of protein and antibody arrays," *Nat Rev Drug Discov* **5**(4), 310–320 (2006).
- [3] Bjerketorp, J., Hakansson, S., and al., S. B., "Advances in preservation methods: keeping biosensor microorganisms alive and active," *Curr Opin Biotechnol* **17**(1), 43–49 (2006).
- [4] Hill, J. J., Shalaev, E. Y., and Zografi, G., "Thermodynamic and dynamic factors involved in the stability of native protein structure in amorphous solids in relation to levels of hydration," *J. Pharm. Sci.* **94**(8), 1636–1667 (2005).
- [5] Ehrnsperger, M., Hergersberg, C., et al., "Stabilization of proteins and peptides in diagnostic immunological assays by the molecular chaperone hsp25," *Analytical Biochemistry* **259**(2), 218–225 (1998).
- [6] Roy, I. and Gupta, M. N., "Freeze-drying of proteins: some emerging concerns," *Biotechnol Appl Biochem* **39**, 165–77 (2004).
- [7] Fonseca, F., Cenard, S., and Passot, S., "Freeze-drying of lactic acid bacteria," *Methods Mol Biol* **1257**, 477–88 (2015).
- [8] Wang, S., Goecke, T., and al., C. M., "Freeze-dried heart valve scaffolds," *Tissue Engineering Part C-Methods* **18**(7), 517–525 (2012).
- [9] Wang, S., Oldenhof, H., and al., T. G., "Sucrose diffusion in decellularized heart valves for freeze-drying," *Tissue Engineering Part C-Methods* **21**(9), 922–931 (2015).
- [10] Wang, W., "Lyophilization and development of solid protein pharmaceuticals," *International Journal of Pharmaceutics* **203**(1), 1–60 (2000).
- [11] Arakawa, T., Prestrelski, S., et al., "Factors affecting short-term and long-term stabilities of proteins," *Advanced drug delivery reviews* **46**, 1–3 (2001).
- [12] Carpenter, J., Hand, S., et al., "Cryoprotection of phosphofructokinase with organic solutes: characterization of enhanced protection in the presence of divalent cations," *Archives of Biochemistry and Biophysics* **250**, 505–512 (1986).
- [13] Carpenter, J. and Crowe, J., "The mechanism of cryoprotection of proteins by solutes, cryobiology," *Cryobiology* **25**, 244–255 (1988).

- [14] “Protein purification.” <https://www.embl.org/groups/protein-expression-purification/services/protein-purification/> (Feb 2022).
- [15] Young, M. A., Antczak, A. T., Wawak, A., Elliott, G. D., and Trammell, S. R., “Light-assisted drying for protein stabilization,” *Journal of Biomedical Optics* **23**(7), 075007 (2018).
- [16] Young, M. A., Furr, D. P., McKeough, R. Q., Elliott, G. D., and Trammell, S. R., “Light-assisted drying for anhydrous preservation of biological samples: optical characterization of the trehalose preservation matrix,” *Biomedical Optics Express* **11**(2), 801–816 (2020).
- [17] Clegg, J. S., “Cryptobiosis a peculiar state of biological organization,” *Comparative Biochemistry and Physiology Part B: Biochemistry and Molecular Biology* **128**(4), 613–624 (2001).
- [18] Yu, L., “Amorphous pharmaceutical solids: preparation, characterization and stabilization,” *Advanced Drug Delivery Reviews* **48**(1), 27–42 (2001).
- [19] Crowe, J. and Crowe, I., “Preservation of mammalian cells, learning of nature tricks,” *Nat Biotechnol* **18**, 145–147 (2000).
- [20] Welniczab, W. et al., “Anhydrobiosis in tardigrades the last decade,” *Journal of Insect Physiology* **57**(5), 577–583 (2011).
- [21] Einfal, T. et al., “Methods of amorphization and investigation of the amorphous state,” *Acta pharmaceutica* **63**(3), 305–334 (2013).
- [22] “Comparison of various milling technologies for grinding pharmaceutical powders,” *International Journal of Mineral Processing* **74**, S173–S181 (2004). Special Issue Supplement Comminution 2002.
- [23] “Perspectives on the amorphisation/milling relationship in pharmaceutical materials,” *Advanced Drug Delivery Reviews* **100**, 51–66 (2016).
- [24] Millqvist-Fureby, A., Malmsten, M., and Bergenstahl, B., “Spray-drying of trypsin â surface characterisation and activity preservation,” *International Journal of Pharmaceutics* **188**(2), 243–253 (1999).
- [25] Elliott, G. D., Chakraborty, N., and Biswas, D., “Anhydrous preservation of mammalian cells: cumulative osmotic stress analysis,” *Biopreservation and biobanking* **6**(4), 253–260 (2008).
- [26] Wolkers, W., “From anhydrobiosis to freeze-drying of mammalian cells,” *Comparative Biochemistry and Physiology, Part A* (126), S159 (2000).
- [27] Crowe, L. M., Crowe, J. H., Rudolph, A., Womersley, C., and Appel, L., “Preservation of freeze-dried liposomes by trehalose,” *Archives of biochemistry and biophysics* **242**(1), 240–247 (1985).

- [28] Fedorov, M. V., Goodman, J. M., Nerukh, D., and Schumm, S., “Self-assembly of trehalose molecules on a lysozyme surface: the broken glass hypothesis,” *Physical chemistry chemical physics* **13**(6), 2294–2299 (2011).
- [29] Allison, S. et al., “Hydrogen bonding between sugar and protein is responsible for inhibition of dehydration-induced protein unfolding,” *Arch. Biochem. Biophys* **365**, 289–298 (1999).
- [30] Massari, A. M., Finkelstein, I. J., McClain, B. L., Goj, A., Wen, X., Bren, K. L., Loring, R. F., and Fayer, M. D., “The influence of aqueous versus glassy solvents on protein dynamics: Vibrational echo experiments and molecular dynamics simulations,” *Journal of the American Chemical Society* **127**(41), 14279–14289 (2005).
- [31] Lerbret, A., Affouard, F., Bordat, P., Hedoux, A., Guinet, Y., and Descamps, M., “Low-frequency vibrational properties of lysozyme in sugar aqueous solutions: A raman scattering and molecular dynamics simulation study,” *The Journal of chemical physics* **131**(24), 12B620 (2009).
- [32] Champion, D., Le Meste, M., and Simatos, D., “Towards an improved understanding of glass transition and relaxations in foods: molecular mobility in the glass transition range,” *Trends in food science & technology* **11**(2), 41–55 (2000).
- [33] Chen, T., Fowler, A., and Toner, M., “Literature review: supplemented phase diagram of the trehalose–water binary mixture,” *Cryobiology* **40**(3), 277–282 (2000).
- [34] Brostow, W., Chiu, R., Kalogerias, I. M., and Vassilikou-Dova, A., “Prediction of glass transition temperatures: Binary blends and copolymers,” *Materials Letters* **62**(17-18), 3152–3155 (2008).
- [35] Furr, D., Lam, P. A., Tran, A., McKeough, R. Q., Beasock, D., Chandler, M., Afonin, K. A., and Trammell, S. R., “Thermal stabilization of nuclei acid nanoparticles (nanps) using light-assisted drying,” in [*Colloidal Nanoparticles for Biomedical Applications XVI*], **11659**, 1165913, International Society for Optics and Photonics (2021).
- [36] Abazari, A., Chakraborty, N., Hand, S., et al., “A raman microspectroscopy study of water and trehalose in spindried cells,” *Biophysical journal* **107**(10), 2253–2262 (2014).